Journal of Business, Social and Technology
Volume 7, Issue 1, 56-67
e_ISSN: 2807-6362
https://bustechno.polteksci.ac.id/index.php/jbt/index
DOI : doi.org/10.59261/jbt.vxix.584

Evaluation of Support Reactions on a Floating Breakwater Moored by a Catenary System: Effects of Fairlead Position Variations

***Hotma Harapan Saragih[1]**
Universitas Tarumanagara, Indonesia

Roesdiman Sogiarso[2]
Universitas Tarumanagara, Indonesia

Indra Noer Hamdhan[3]
Institut Teknologi Nasional, Indonesia

***Corresponding author:**
Hotma Harapan Saragih, Universitas Tarumanagara, Indonesia.
✉saragih.hotma@gmail.com

Article Info:

Article history:
Received: December 01, 2026
Revised: January 04, 2026
Accepted: February 07, 2026

Keywords:
catenary mooring system; floating breakwater; fairlead position; sap2000; support reactions

Abstract

Background: Floating breakwaters are widely applied in medium-depth waters, where performance depends on catenary mooring and fairlead position. Variations in fairlead elevation and chain angle alter support force distribution, yet systematic parametric evaluation of support reactions remains limited.
Objective: This study aims to analyze support reactions on a 55 × 30 × 10 m floating breakwater moored by a 10-line studlink chain catenary system, focusing on the effects of fairlead elevation (z = −5, 0, +5 m) and chain angle variations (θ = 7.5°–15°) on horizontal and vertical force distribution at supports.
Method: A finite element analysis was conducted using SAP2000. The model incorporated structural geometry, pretension forces, buoyancy, hydrodynamic loads, wind loads, and defined load combinations. Support reactions in X, Y, and Z directions were extracted for each fairlead and angle configuration. Parametric comparisons were performed to identify critical supports and peak reaction trends.
Result: The horizontal X component dominated support reactions (≈240–276 MN) and increased with chain angle θ. The Y component (≈37–112 MN) showed similar trends but lower magnitude. The vertical Z component was highly sensitive to fairlead elevation, with lower z values producing uplift and higher elevations causing downward forces. Sign changes in Z indicate different supportage failure modes depending on fairlead configuration.
Conclusion: Fairlead elevation and catenary geometry significantly influence support reaction distribution. These parameters must be carefully optimized to ensure structural safety and adequate supportage capacity in floating breakwater design.

To cite this article: Saragih, H. H., Sogiarso, R., & Hamdhan, I. N. (2026). Evaluation of support reactions on a floating breakwater moored by a catenary system: Effects of fairlead position variations. *Journal of Business, Social and Technology, 7*(1), 56–67. https://doi.org/10.59261/jbt.v7i1.584

INTRODUCTION

Floating wave breakers (floating breakwater) have developed as an effective engineering solution for coastal and harbor protection by damping wave energy in medium- to deep-depth waters, where conventional construction methods (land-based revetment and breakwater) have become less economical or impractical. Floating structures offer a variety of advantages, including high mobility, relatively short installation times, and adaptability to water level variations (Amaechi et al., 2022; Huebner, 2025). Recent studies have also shown that the effectiveness of

wave attenuation is greatly influenced by the configuration of its structure and mooring system (Luo et al., 2025; Tay & Lin Htoo, 2025; Vishwakarma & Karmakar, 2024). However, the hydrodynamic characteristics and operational stability of floating breakwater are greatly influenced by the mooring system that holds the structure against wave forces, wind, and currents (Samuel et al., 2025). Therefore, the design of the mooring system is a key aspect to ensure the function of wave attenuation while ensuring the safety of the structure and supportage capacity on the seabed, as also recommended in the international mooring design standards (Wang, 2022).

Previous research has shown a number of important points related to the interaction between floating breakwater and mooring systems (Dai et al., 2018). In the context of hydrodynamics, the response of floating structures to waves (amplitude of motion, phase, and damping) is influenced by the mass of inertia, the geometry of the pontoon, as well as the mooring interactions that regulate the degree of freedom of motion (heave, surge, sway, roll, pitch, yaw). Newman (2018) and Yang (2019) discuss the basic theory of floating structure hydrodynamics as well as the importance of modeling added mass and viscous damping to predict dynamic responses. Coupled numerical analysis also shows that the nonlinear interaction between the structure and mooring under random waves requires a fully coupled dynamic analysis approach to obtain an accurate response (Li et al., 2024). In addition, uncertainty in mooring parameters can affect the overall reliability of the structure, so the reliability analysis of the system becomes important in the design stage (Hou et al., 2019).

Experimental studies have confirmed that the angle of the mooring line (θ) at the fairlead affects the force distribution along the mooring chain and on the support (Barrera et al., 2019). For small θ values, the horizontal component is dominant, but the vertical component remains significant if the pretension is high. For large θ values, the increase in horizontal components can magnify the lateral moment and force on a particular support, thus making that support more critical. Numerical analysis of catenary systems and their variations also shows significant differences in tension distribution and dynamic response due to changes in geometric configurations (Konispoliatis & Mavrakos, 2025; Manolas et al., 2025).

Nonlinear effects such as chain contact with the seafloor, ground friction, and viscous wave interactions can produce significant differences compared to potential theory-based linear predictions, so a combination of dynamic numerical analysis, soil capacity verification, and specialized software-based simulations such as OrcaFlex is often recommended for the final design stage (Touzón González, 2021; Yan et al., 2025). In addition, extending the fatigue life of the mooring system is also an important concern in the context of long-term cyclic loads (Shahrabi & Bargi, 2019; Wei et al., 2026).

In the context of this study, a floating breakwater model measuring (55 × 30 × 10) m tethered with 10 catenary studlink chains was analyzed with variations in fairlead elevation (z = −5, 0, 5 m) and uniform mooring angle variations θ (7.5°–15°). The analysis uses SAP2000 to generate support reactions on each support for the X, Y, and Z force components, thus allowing the evaluation of the effect of the combination of catenary geometry, pretension, and wave and wind loads on the force distribution to the supportage system. This approach is in line with the integrated numerical analysis practices commonly used in the dynamic response study of modern floating structures (Pimenta et al., 2020).

Based on the background outlined above, this study aims to (1) present the results of the baseline reactions for all test combinations, (2) identify the most critical supports in each combination, and (3) provide design recommendations and further verification needs based on numerical findings and comparisons with previous studies and industry standard practices. This will contribute to the optimization of the mooring system design, ensuring the stability and efficiency of the floating breakwater in real-world applications.

LITERATURE REVIEW

Understanding the mechanisms of wave energy reduction by breakwater structures—both conventional and floating—is rooted in the concepts of wave energy and wave–structure interaction. For periodic linear waves, the energy per unit crest length is expressed by the classical equation $E = \frac{1}{8}\rho g H^2$, where ρ is the density of seawater, g is the acceleration due to gravity, and

H is the wave height (Newman, 2018). The magnitude of this energy is the basis for assessing how much energy is reflected, absorbed, or transmitted by an obstacle in the wave's path.

The transmission coefficient K_t is defined as the ratio of the transmitted wave height to the incoming wave height, i.e., $K_t = \frac{H_t}{H_i}$. The relationship between the transmission coefficient and the transmitted energy ratio T_r is given by $T_r = {K_t}^2$. Thus, the percentage of energy reduction achieved by the structure is $(1 - T_r)x100\% = \left(1 - {K_t}^2\right)x100\%$. This relationship provides a quantitative way to compare the wave attenuation effectiveness of different types of structures.

Floating breakwaters attenuate waves through several mechanisms that differ from those of fixed mass-based breakwaters. The main mechanisms include: (1) reflection and diffraction due to the presence of the pontoon body that alters the wave field, (2) energy absorption through relative motion of the structure (radiated waves and hydrodynamic dissipation), (3) viscous energy dissipation around the structural elements, and (4) interaction with the mooring system that affects the amplitude and phase of the structure's motion. Due to the free-motion characteristics of floating breakwaters, some of the wave energy can be converted into kinetic energy of the structure and ultimately dissipated, resulting in a reduction in wave height in the sheltered area.

The effectiveness of floating breakwaters is influenced by a number of design parameters. Relative freeboard (ratio of freeboard to H), draft (submerged depth), frontal shape of the pontoon, and structural porosity determine the extent to which waves are reflected or transmitted. Empirically, the transmission coefficient can often be modeled as an exponential function of the freeboard ratio—for example, $K_t = \exp\left(-\alpha\frac{F}{H}\right)$—where α is a constant that depends on the geometry and surface characteristics of the structure (values of α are obtained from experimental tests). In addition, the mooring configuration—including chain type (studlink), chain length, pretension, and especially fairlead elevation—determines the distribution of horizontal and vertical forces transmitted to the support and influences the dynamic response of the structure.

Experimental and numerical literature supports the assertion that floating breakwaters can function similarly to conventional breakwaters in terms of wave energy reduction when the pontoon design and mooring system are optimized. Laboratory tests and simulations show that with appropriate freeboard, draft, and pontoon geometry, along with a proper mooring arrangement (pretension and fairlead elevation), the transmission coefficient can be reduced to values equivalent to those of a number of rigid structures under certain wave conditions (Newman, 2018). However, relative effectiveness also depends on the wave period: floating breakwaters tend to be more effective over a medium period range because of the dynamic response of the structure (resonance, radiated waves) that plays a significant role.

Several practical aspects require attention in design and implementation. First, nonlinear effects—including viscous damping, contact chain interactions, and their impact on energy dissipation—often cause practical results to differ from simple linear predictions; therefore, a combination of analytical methods and laboratory tests is recommended. Second, catenary mooring systems generate large vertical and horizontal force components on the support; different fairlead elevations can change the sign and magnitude of the vertical force (uplift vs. downpull), so the subgrade capacity analysis and support design must take both conditions into account.

Based on the theoretical basis and literature findings, this paper continues with a numerical analysis of the support reactions on a floating breakwater moored using a catenary system. Prior studies on floating breakwater mooring systems have predominantly examined global performance metrics such as wave transmission coefficients and peak mooring line tensions under simplified loading conditions. However, a systematic parametric evaluation of the directional support support reaction components—particularly the influence of fairlead elevation (z) on the sign and magnitude of vertical Z-reactions under combined operational loading—remains insufficiently addressed.

This gap is critical because Z-force sign reversal (uplift vs. downward pull) has direct and differing implications for support foundation design. No study in the reviewed literature has simultaneously examined the interaction between fairlead elevation (z = −5, 0, +5 m) and rope

angle (θ = 7.5°–15°) on all three reaction components (X, Y, Z) under a full combined load case. The present study addresses this gap by generating a quantitative parametric design envelope for a 55×30×10 m floating breakwater pontoon using FEA in SAP2000 with a stud-link chain catenary system, for various fairlead elevations and rope angles. The objectives of the analysis are to quantify the force distribution at the supports, identify critical conditions with respect to angle and elevation, and assess the extent to which the mooring configuration affects the wave attenuation capability and structural support design requirements.

METHOD

This study aims to calculate and analyze the support reactions on a floating breakwater measuring (55 × 30 × 10) m, moored using a stud link chain catenary system of 10 segments (5 on the left side and 5 on the right side). The analysis focuses on the influence of fairlead elevation (z = −5 m, z = 0 m, z = 5 m) and variations in the uniform line angle θ (θ = 7.5°; 7.63°; 8°; 10°; 12°; 13°; 15°) on the distribution of support reactions on each support.

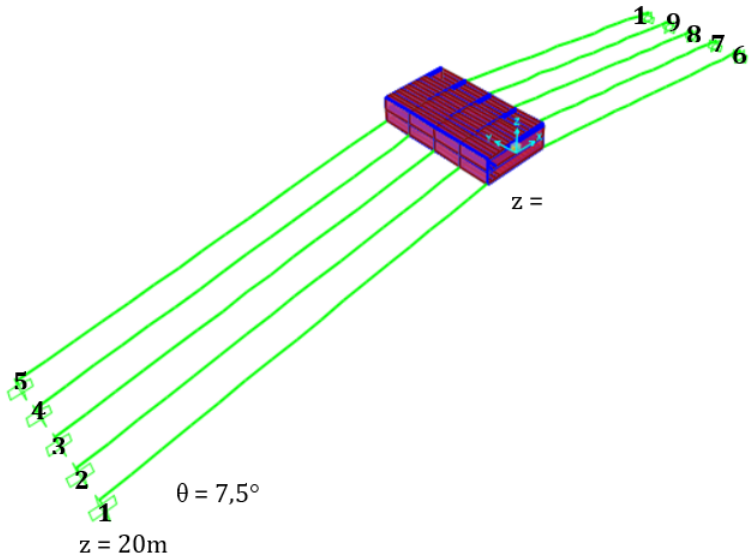

Figure 1. Model (60 x 30 x 10) m where the fairlead is at a height z = -5m

Table 1. Coordinate Support

Fairlead position on z		-5	
0		7,5⁰	
Support No. (Author)	X	Y	Z
1	-166,92	0	-25
2	-166,92	13,75	-25
3	-166,92	27,5	-25
4	-166,92	41,25	-25
5	-166,92	55	-25
6	-166,92	0	-25
7	-166,92	13,75	-25
8	-166,92	27,5	-25
9	-166,92	41,25	-25
100	-166,92	55	-25

Fairlead position on z		-5	
0		7,5⁰	
Support No. (Author)	X	Y	Z
1	-166,28	0	-25
2	-166,28	13,75	-25
3	-166,28	27,5	-25
4	-166,28	41,25	-25
5	-166,28	55	-25
6	-166,28	0	-25
7	-166,28	13,75	-25
8	-166,28	27,5	-25
9	-166,28	41,25	-25
100	-166,28	55	-25

The steps of the methodology carried out are explained as follows:

First, preparation of model and loading parameters. The geometric model of the floating breakwater body is compiled in accordance with the specifications of the study, with dimensions of a length of 55 m, a width of 30 m, a height of 10 m, and an effective draft of 5 m. The fairlead points and support coordinates (seabed at z = −25 m) are defined and numbered consistently. The

loading parameters used are: dead load D = 42.2 kN/m^2 (based on heavy construction of 1,351.2 tons and sand ballast of 7,105.1 tons), live load L = 14.65 kN/m^2, peak hydrodynamic component HRZ_peak = 10.1 kN/m^2, wind load = 0.5 kN/m^2, buoyancy B = 50.28 kN/m^2, and pretension per mooring line PRET = 666.667 kN. The wave conditions used as reference are H = 2.5 m, T = 5.5 s, and wave velocity V = 122.9 cm/s. The load combinations analyzed follow the design formulas that have been determined: Comb1 = 1.1D + 1.1L + 1.25HRZ_peak + 1.25Wind − 1.1B and Comb2 = 1.1D + 1.25Wind + 1.0PRET − 1.1B.

Second, numerical modeling in SAP2000. The structural model and mooring system are implemented. The pontoon body is modeled using appropriate rod/plate elements with the specified geometry; fairlead nodes are defined at the specified locations and elevations. Mooring lines (stud link chains) are modeled as cable elements or elements that represent the chain characteristics with mass per unit length and appropriate stiffness. Pretension is entered as an initial force on the cable elements, except when modeling limitations of pretension force are addressed through equivalent force substitution at the fairlead node. Boundary conditions for the supports are applied at the seabed coordinates (z = −25 m) to record support reactions. Distributed loads (D, L, HRZ_peak, Wind, B) are applied to the pontoon body according to the projected area; if required, loads are distributed to elements/nodes in accordance with the mesh to ensure accurate load representation.

Third, case analysis and calculation procedures. Analysis is performed for all combination cases for each specified value of θ with fairlead elevations z of −5 m and 0.5 m, respectively. If SAP2000 produces reaction output separated for each load component (e.g., reaction due to D, reaction due to HRZ_peak, reaction due to Wind, reaction due to PRET), then the reaction per support for load combinations (Comb1 and Comb2) is calculated by combining the component reactions using the combination coefficients that have been set. If the output is only available as the total reaction for a given load condition, verify that the load combination is not duplicated (e.g., pretension is not entered twice).

Fourth, data processing and analysis. Reaction results per support for each case are extracted and compiled in a table containing the X, Y, and Z components in MN units. From the dataset, the absolute peak per component is identified, as well as the critical supports for each combination of θ and z. Trend plots are then generated to visualize the change in support reactions with variation of θ for each fairlead elevation, namely graphs of X vs. θ, Y vs. θ, and Z vs. θ (with separate lines per z). In addition, top-view and side-view maps are generated showing support coordinates and critical support annotations to facilitate interpretation of the spatial distribution of reactions. All graphs and tables are included in the main script.

Fifth, model verification, validation, and sensitivity analysis. Verification steps include checking unit consistency (MN confirmation), axis sign convention, and inspection of the reaction force source in the SAP2000 output (to confirm whether the large Z value represents the force per support or an aggregated result). If the vertical values show extreme magnitudes, further checking is carried out on pretension modeling, node aggregation, load placement, and additional fairlead elevation variations to test the sensitivity of vertical behavior transitions.

Sixth, reporting and documentation. Every step of the modeling and results analysis is documented in detail, including SAP2000 input files, support coordinate tables, and reaction output files. All reaction results per support for all cases are arranged so that they can be checked, reused, and used for support capacity calculations and further geotechnical studies. The recommended final output to be included in the script covers a summary table of peak reactions, X/Y/Z trend graphs vs. θ per z, support position schematics, technical interpretation, and recommendations for verification and design.

Workflow (Flowchart). The study workflow follows sequential stages: (1) preparation of data and loading parameters; (2) creation of geometric models and definition of supports and fairleads; (3) definition of mooring element properties and pretension; (4) load input and load combinations; (5) implementation of analysis in SAP2000 for each case of θ and z; (6) extraction of reactions per support; (7) processing and visualization of results.

RESULTS AND DISCUSSION

Results

Analysis results of the support reactions obtained from the SAP2000 model for a floating breakwater (55 × 30 × 10) m, with an effective draft of 5 m, are presented and discussed in this section. The analysis was conducted for fairlead elevation variations of z = −5, 0, and 5 m, and uniform rope angle variations of θ = 7.5°, 7.63°, 8°, 10°, 12°, 13°, and 15°. All support reactions are reported in meganewton (MN) units and are compiled in Table 2 (a complete table of reactions per support for every combination).

Table 2. Calculation Results Structure

No	Support Reaction		MU1A (55 x 30 x 10) - submerged 5 m											
			θ = 7.5°											
			n = 10											
			z = -5				z = 0				z = 5			
			1	5	6	7	1	5	7	10	1	2	5	7
1	Horizontal - X (MN)	(+)				248.46			243.79					248.15
		(-)		-249.74				-245.04					-247.08	
2	Horizontal - Y (MN)	(+)		56.19						43.86			37.20	
		(-)	-56.20				-43.86				-37.20			
3	Vertical (MN)	(+)	147,576.05					15,984.79						41,660.49
		(-)			-147,547.7					-15,956.42		-41,632.13		

No	Support Reaction		MU1A (55 x 30 x 10) - submerged 5 m											
			θ = 7.63°											
			n = 10											
			z = -5				z = 0				z = 5			
			1	5	6	9	1	5	7	10	1	2	5	7
1	Horizontal - X (MN)	(+)				248.50			242.7					248.5
		(-)		-249.84				-244.0					-247.4	
2	Horizontal - Y (MN)	(+)		57.22						44.4			37.9	
		(-)			-57.22		-44.4				-37.9			
3	Vertical (MN)	(+)	200,115.94					13,226.8						53,766.1
		(-)			-200,087.					-13,198.4		-53,737.7		

No	Support Reaction		MU1A (55 x 30 x 10) - submerged 5 m											
			θ = 8°											
			n = 10											
			z = -5				z = 0				z = 5			
			1	5	6	9	1	5	7	10	1	4	5	7
1	Horizontal - X (MN)	(+)				248.12			240.49					248.26
		(-)		-249.64				-242.08					-246.96	
2	Horizontal - Y (MN)	(+)		59.93						45.94			39.72	
		(-)	-59.93				-45.94				-39.72			
3	Vertical (MN)	(+)	161,912.10					9,889.40						48,878.88
		(-)			-161,883.70					-9,861.06		-48,850.53		

No	Support Reaction		MU1A (55 x 30 x 10) - submerged 5 m											
			θ = 10°											
			n = 10											
			z = -5				z = 0				z = 5			
			1	5	6	7	1	3	5	6	1	2	5	7
1	Horizontal - X (MN)	(+)				254.19				237.49				256.18
		(-)	-257.12					-232.60			-252.26			
2	Horizontal - Y (MN)	(+)		74.78					53.85				49.61	
		(-)	-74.78				-53.85				-49.61			
3	Vertical (MN)	(+)	181,956.91							4,387.89				58,747.08
		(-)			-181,928.52		-4,359.91					-58,718.73		

No	Support Reaction		MU1A (55 x 30 x 10) - submerged 5 m											
			θ = 12°											
			n = 10											
			z = -5				z = 0				z = 5			
			1	5	6	7	1	3	6	10	1	2	5	7
1	Horizontal - X (MN)	(+)				261.37			262.74					266.04

		(-)	-266.71						-256.16				-259.80				
2	Horizontal - Y (MN)	(+)		89.58							70.17				59.51		
		(-)	-89.58				-70.17						-59.51				
3	Vertical (MN)	(+)	231,122.86							22,562.37						82,284.46	
		(-)		-231,094.49			-22,534.12							-82,256.12			

No	**Support Reaction**		**MU1A (55 x 30 x 10) - submerged 5 m**											
			θ = 13°											
			n = 10											
			z = -5				**z = 0**			**z = 5**				
			1	**5**	**6**	**7**		**1**	**5**	**4**	**7**			
1	Horizontal - X (MN)	(+)				263.39					269.61			
		(-)	- 270.25					-261.88						
2	Horizontal - Y (MN)	(+)		96.93					64.41					
		(-)	- 96.93					-64.41						
3	Vertical (MN)	(+)	251,585.36								89,665.59			
		(-)			-251,556.99					-89,637.26				

No	**Support Reaction**		**MU1A (55 x 30 x 10) - submerged 5 m**															
			θ = 15°															
			n = 10															
			z = -5				**z = 0**				**z = 5**							
			1	**5**	**6**	**7**	**1**	**3**	**6**	**10**	**1**	**2**	**5**	**7**				
1	Horizontal - X (MN)	(+)				265.09			274.08					275.16				
		(-)	-275.76					-262.38			-263.71							
2	Horizontal - Y (MN)	(+)		111.55						88.61			74.16					
		(-)	-111.55				-88.61				-74.16							
3	Vertical (MN)	(+)	286,439.27						63,208.14					107,059.21				
		(-)			-		-					-						

	286,4 10.91	63,1 79.84	107,0 30.89

Discussion

Peak analysis summary shows that the horizontal component in the X direction dominates the support reactions for almost all cases. The maximum positive X value recorded is 275.76 MN at θ = 15° and z = −5 m (Support 5). Generally, the X values in the studied cases range from approximately 240–276 MN, with a trend of increasing X along with increasing θ. The lateral component Y has a smaller magnitude than X, ranging from approximately 37–112 MN; the maximum Y value recorded is approximately 111.55 MN for the case θ = 15°. The vertical component Z shows the most complex and varied behavior: Z values can be either large positive (upward pull) or large negative (downward pull), with extreme positive values up to approximately 286,439.27 MN (case θ = 15°, z = −5 m) and extreme negative values down to approximately −107,030.89 MN (cases θ = 15°, z = 5 m).

Influence of Rope Angle θ and Fairlead Elevation z. The results show two main effects: (1) increasing the chain angle θ increases the transmitted horizontal components (X and Y) to the support; (2) the fairlead elevation z greatly influences the sign and magnitude of the vertical component Z. Quantitatively, for z = −5 m and increasing θ from 7.5° to 15°, there is an increase in X from approximately 248 MN to approximately 276 MN at the critical support. This behavior is consistent with catenary geometry: a greater angle induces higher pretension and hydrodynamic loading, resulting in larger horizontal components and thus a greater lateral pull on the support.

For the Z component, a low fairlead elevation (z = −5 m) tends to produce large positive Z values (uplift at the support), while a high fairlead elevation (z = 5 m) often produces negative Z values (downward pull or compression). The change in sign is a result of the displacement geometry of the mooring line and the directional consequence of the difference in relative fairlead position with respect to the centroid of the structure and the hydrodynamic loading point. Dramatic changes in the sign of Z for certain parameter combinations confirm that fairlead elevation must be treated as a critical design parameter, given its significant impact on the support failure mode (uplift *vs.* pullout).

Distribution pattern among supports and critical support identification: The support position mapping (Table 1) shows that the support on the left side (Support 5) and several right-side supports (depending on the case) often appear as critical supports, especially for components X and Z. For example, at θ = 7.5°, Support 5 shows X ≈ 248.5 MN and Z ≈ 147.576 MN (positive) for z = −5, whereas at θ = 15°, Support 5 shows X ≈ 275.76 MN and Z ≈ 286.439 MN (positive). Critical support identification was performed based on marking the absolute peak of each component across all cases; a summary table of peaks and a map of critical support locations are included in Table 2 and Figure 1 (schematic top/side view).

Comparison of SAP2000 Reactions with Theoretical Load Combination Results (Comb1/Comb2). Calculation of load combinations at the pressure level produces a distributed total: Comb1 ≈ 20.477 kN/m^2 → total ≈ 33.793 kN (≈ 33.793 MN) for a projection area of 1,650 m^2; Comb2 (partially distributed) ≈ −8.263 kN/m^2 → total ≈ −13.634 kN, plus a total PRET of 666.667 kN → net ≈ −12.967 MN. These combination values are relatively small when compared to the reactions per support reported by SAP2000 (tens to hundreds of MN). This large discrepancy indicates that the SAP2000 output analyzed may already contain other large force components — for example, the aggregation of distributed structural loads, internal pretension contributions, or hydrostatic effects modeled on nodes/elements in a cumulative manner. Therefore, to accurately calculate the combined reaction per support, separated reaction outputs are required for each loading component (D, L, HRZ*peak*, Wind, PRET) so that combination coefficients can be applied at the level of each individual component.

Data Validity and Requirements. Verify the vertical Z-value with a magnitude of hundreds of thousands of MN, which must be verified before being used as a basis for design. Possible sources of discrepancy or extreme values include: (a) SAP2000 displays aggregate results from multiple nodes/elements such that the numbers reflect an incomplete summation distributed at the support level; (b) pretension or hydrostatic loads were entered more than once; (c) units or

number formats were converted incorrectly during the recapitulation of results. Therefore, we recommend the following verification steps: extraction of reactions per support for each load component separately; inspection of whether the reported figures represent the force on a single support node or an aggregate; and checking the pretension (PRET) input to prevent load duplication. This verification must be completed before interpreting the support capacity and subgrade analysis.

Support Design Implications and Recommendations Based on the reliable results, several design implications can be concluded: 1) The support capacity and connection system must be adjusted to withstand significant horizontal forces (up to ≈ 276 MN) and vertical forces that can change sign (uplift or down-pull). Support design must also consider the second condition. 2) Distributed pretension in the cables plays an important role; pretension variation needs to be analyzed (sensitivity ±20%) to evaluate changes in load on the supports. 3) Foundation capacity (bearing, breakout, and uplift resistance) must be checked geotechnically for critical supports; if the foundation cannot withstand major uplift, alternatives (*e.g.*, added deadweight anchors, use of a different support type, or change of fairlead configuration) are required. 4) It is recommended to perform a dynamic mooring analysis (*e.g.*, using OrcaFlex/AQWA) to complement the static/geometric nonlinear analysis in SAP2000, especially for capturing nonlinear chain behavior, viscous interaction, and time-domain response. 5) The catenary mooring system and fairlead elevation have a strong influence on the reaction distribution at the supports of the floating breakwater. For further publication and design purposes, the authors will include a complete reaction table per support, trend graphs ($X/Y/Z$ vs. θ for each z), as well as support schematics; simultaneously, SAP2000 output verification will be performed per component to ensure the accuracy of vertical reactions before making final design decisions.

CONCLUSION

Based on the SAP2000 support reaction analysis of the 55 × 30 × 10 m floating breakwater with a 5 m effective draft moored by a studlink chain catenary system (10 mooring lines; 5 left and 5 right), it can be concluded that the horizontal X component dominates the support reactions in almost all cases, ranging approximately from 240–276 MN and increasing with larger mooring line angles θ, indicating that mooring line angle is a key parameter in lateral load demand. The lateral Y component is smaller (about 37–112 MN) but still increases with θ and must be considered in connection and load distribution design. The vertical Z component exhibits the greatest variation and changes sign depending on fairlead elevation, where low fairleads (z = −5 m) tend to produce significant uplift forces and high fairleads (z = 5 m) generate downward pull, demonstrating that fairlead elevation critically influences support uplift and bearing conditions. Load concentration is observed at edge supports (e.g., support 5 and several right-side supports), requiring focused geotechnical verification and adequate lateral and vertical bearing capacity design at these critical points.

To enhance reliability and operational safety, several steps are recommended. First, a sensitivity analysis of pretension and catenary geometry is essential, varying pretension (e.g., ±20%) and fairlead elevations (e.g., between −7 m and +7 m with finer increments) to assess the influence of these parameters on force distribution and to define safe operational ranges. Second, static and nonlinear analysis using SAP2000 should be complemented with time-domain dynamic mooring simulations to capture nonlinear chain behavior, seabed contact effects, viscous interactions, and transient responses under waves, currents, and wind, thereby validating peak loads and fatigue cycles. Third, a detailed geotechnical investigation and support capacity assessment (uplift, breakout, lateral resistance) must be conducted based on verified peak forces. Alternative solutions such as larger support mass, ground improvement, suction anchors, or mooring reconfiguration should be considered if soil capacity is insufficient.

Connection components like fairleads, shackles, and support interfaces should be designed with adequate safety factors against combined horizontal and vertical loads, while accounting for fatigue and corrosion effects. Finally, non-uniform mooring line angles and extreme operational scenarios, including storm events or partial mooring failure, should be analyzed to anticipate non-ideal force redistribution under real field conditions. Overall, the catenary configuration, particularly mooring line angle and fairlead elevation, has a decisive influence on

force distribution and must be carefully integrated into mooring and support design to ensure optimal performance and safety in floating breakwater systems.

ACKNOWLEDGEMENT

We would like to express our sincere gratitude to the individuals and institutions that contributed to the completion of this study. Special thanks to Department of Civil Engineering, Universitas Tarumanagara and Institut Teknologi Nasional, Indonesia for their support. We also acknowledge the valuable insights and support provided by Dr. John Doe, Supervisor, Universitas Tarumanagara, whose guidance was instrumental in shaping this research.

AUTHOR CONTRIBUTION STATEMENT

Hotma Harapan Saragih and Roesdiman Sogiarso were involved in the conceptualization, methodology, and supervision of the project. Indra Noer Hamdhan contributed to the data analysis and validation of results. All authors were involved in writing and reviewing the manuscript, and all agreed to the final version for publication.

REFERENCES

Amaechi, C. V., Reda, A., Butler, H. O., Ja'e, I. A., & An, C. (2022). Review on fixed and floating offshore structures. Part I: Types of platforms with some applications. *Journal of Marine Science and Engineering*, *10*(8), 1074.

Barrera, C., Guanche, R., & Losada, I. J. (2019). Experimental modelling of mooring systems for floating marine energy concepts. *Marine Structures*, *63*, 153–180. https://doi.org/10.1016/j.marstruc.2018.08.003

Dai, J., Wang, C. M., Utsunomiya, T., & Duan, W. (2018). Review of recent research and developments on floating breakwaters. *Ocean Engineering*, *158*, 132–151.

Hou, H.-M., Dong, G.-H., Xu, T.-J., & Zhao, Y.-P. (2019). System reliability evaluation of mooring system for fish cage under ultimate limit state. *Ocean Engineering*, *172*, 422–433.

Huebner, S. (2025). Floating and stilted structures as strategies in coastal climate adaptation: Local monsoon adaptation practices and implications for flood risk management. *Climate Risk Management*, *49*, 100719.

Konispoliatis, D. N., & Mavrakos, A. S. (2025). Comparative Analysis of Catenary and TLP Mooring Systems on the Wave Power Efficiency for a Dual-Chamber OWC Wave Energy Converter. *Energies*, *18*(6), 1473. https://doi.org/10.3390/en18061473

Li, W., Du, G., Lin, S., Chuang, Z., & Wang, F. (2024). Dynamic response assessment of floating offshore wind turbine mooring systems with different in-line tensioner configurations based on fully coupled load calculations. *Journal of Marine Science and Engineering*, *12*(12), 2138. https://doi.org/10.3390/jmse12122138

Luo, K., Dong, Y., & Yuan, J. (2025). Impact of mooring configurations on wave attenuation of porous floating breakwater: A comparative experimental study. *Coastal Engineering*, 104823. https://doi.org/10.1016/j.coastaleng.2025.104823

Manolas, D., Konispoliatis, D., Mavrakos, S., & Meleddu, M. (2025). Design and Assessment of Hybrid-Catenary Mooring Systems Using Steel Wire and Polyester Ropes for a 10MW Semi-Submersible and Spar-Buoy Wind Turbine. *International Conference on Offshore Mechanics and Arctic Engineering*, *89282*, V001T01A012. https://doi.org/10.1115/IOWTC2025-164603

Newman, J. N. (2018). *Marine hydrodynamics*. MIT press.

Pimenta, F., Ruzzo, C., Failla, G., Arena, F., Alves, M., & Magalhães, F. (2020). Dynamic response characterization of floating structures based on numerical simulations. *Energies*, *13*(21), 5670.

Samuel, S. P., Gayathri, R., Koley, S., & Muthusamy, C. (2025). Motion responses with hydrodynamic factors in designing a floating breakwater and wave energy converter: a review. *Journal of Ocean Engineering and Marine Energy*, *11*(1), 233–263.

Shahrabi, M., & Bargi, K. (2019). Enhancement the fatigue life of floating breakwater mooring system using tuned liquid column damper. *Latin American Journal of Solids and Structures*, *16*, e220. https://doi.org/10.1590/1679-78255692

Tay, Z. Y., & Lin Htoo, N. (2025). Performance and Wave Attenuation of Stepped-Type Floating Breakwater Under Influence of Mooring Stiffness for Tropical Climate. *International Conference on Offshore Mechanics and Arctic Engineering*, *88964*, V007T12A009. https://doi.org/10.1115/OMAE2025-156243

Touzón González, I. (2021). *Numerical appoaches for loads and motions assessment of floating offshore renewable energy devices moored by means of catenary mooring systems.*

Vishwakarma, R. D., & Karmakar, D. (2024). Hydrodynamic analysis of different shapes of moored hybrid floating breakwater. *Journal of Marine Science and Application*, *23*(4), 743–761. https://doi.org/10.1007/s11804-024-00519-x

Wang, H. (2022). Design of Mooring System. In *Encyclopedia of Ocean Engineering* (pp. 314–319). Springer.

Wei, C., Liu, Y., Huang, S., Xue, G., Yuan, Z., & Li, M. (2026). Impact of parabolic breakwater on the safety characteristics of shared mooring floating oscillating water column devices array under freak waves. *Energy*, 140336. https://doi.org/10.1016/j.energy.2026.140336

Yan, J., Fan, J., Huang, J., & Fang, H. (2025). Dynamic response and fatigue damage of catenary mooring cables based on ANCF. *Proceedings of the Institution of Mechanical Engineers, Part C: Journal of Mechanical Engineering Science*, *239*(8), 2774–2790. https://doi.org/10.1177/09544062241302235

Yang, J., He, E. M., & Hu, Y. Q. (2019). Dynamic modeling and vibration suppression for an offshore wind turbine with a tuned mass damper in floating platform. *Applied Ocean Research*, *83*, 21–29.